

Chiral symmetry and the nucleon's vector strangeness form factors

M. J. Ramsey-Musolf^{1,*} and Hiroshi Ito²

¹*Institute for Nuclear Theory, University of Washington, Seattle, Washington 98195*

²*Center for Nuclear Studies, Department of Physics, George Washington University, Washington, D.C. 20052*

(Received 15 July 1996)

The nucleon's strange-quark vector current form factors are studied from the perspective of chiral symmetry. It is argued that chiral perturbation theory cannot yield a prediction for the strangeness radius and magnetic moment. Arrival at definite predictions requires the introduction of additional, model-dependent assumptions which go beyond the framework of chiral perturbation theory. A variety of such model predictions is surveyed, and the credibility of each is evaluated. [S0556-2813(97)00206-9]

PACS number(s): 14.20.Dh, 11.30.Rd, 12.40.-y

I. INTRODUCTION

There has been considerable interest recently in the strange quark "content" of the nucleon [1–15]. The reasons for this interest are both theoretical and phenomenological. In the latter case, early analyses of the pion-nucleon sigma term [16] and later results for the nucleon's inclusive, spin-dependent deep-inelastic structure functions [17–21] suggested that a nontrivial fraction of the nucleon's mass and spin are carried by the $s\bar{s}$ component of the sea. Subsequent analyses of the sigma term have reduced the value of $\langle p|\bar{s}s|p\rangle/\langle p|\bar{u}u+\bar{d}d|p\rangle$, and therefore the strange-quark contribution to m_N , by a factor of 2 [22], while studies of SU(3) breaking in the axial vector octet imply a theoretical uncertainty in the value of Δs , the strange quark contribution to the nucleon's spin extracted from deep-inelastic scattering (DIS) measurements, sufficiently large to make the bounds on Δs consistent with zero [23–26]. Nevertheless, the early analyses of the sigma term and polarized DIS results have motivated proposals to measure another strange-quark observable, $\langle p|\bar{s}\gamma_\mu s|p\rangle$. Indeed, several low- and medium-energy parity-violating electron scattering experiments are either underway or planned at MIT-Bates [2,3], TJNAF [4–6], and Mainz [7] with the goal of measuring the two form factors which parametrize the nucleon's strange-quark vector current, $G_E^{(s)}$ and $G_M^{(s)}$.

Theoretically, strange quarks are interesting because they do not appear explicitly in most quark model descriptions of the nucleon. Although the quark model provides a useful intuitive picture of the nucleon's substructure and has seen considerable success in accounting for a wide range of properties of the low-lying hadrons [27], one knows that there is more to the nucleon than the three constituent quarks. In particular, processes such as DIS and Drell-Yan have provided considerable insight regarding the important role played by the $q\bar{q}$ and gluon sea when the nucleon interacts at high energies [8]. Almost no information exists, however, regarding the low-energy manifestations of the sea. Because strange quarks constitute purely sea degrees of freedom, low-

and intermediate-energy determinations of strange-quark matrix elements offer a new window on the "low-energy" structure of the nucleon which goes beyond the description provided by the quark model. In particular, the weak neutral current scattering experiments mentioned above should set bounds on the spatial polarization of the $s\bar{s}$ sea [4,6], its contributions to the nucleon magnetic moment [2–4] and spin [9], and its role in the nuclear response at moderate momentum transfer [5].

One has seen considerable progress over the past few years in clarifying the interpretation of neutral current observables in terms of strangeness matrix elements [1,10–13]. The situation regarding theoretical predictions for these matrix elements is less advanced. Ideally, one would hope to draw inferences from the deep-inelastic data on s and \bar{s} distributions [28] for elastic vector and axial vector strangeness matrix elements. However, the high-energy data provide light-cone momentum distribution functions, and one does not know at present how to translate this information into the spin and spatial nucleon wave functions as needed to compute charge radii, magnetic moments, etc. [29]. Similarly, one might hope for first-principles microscopic predictions using lattice QCD. To date, lattice results for the strangeness axial charge [14] and strangeness magnetic moment [15] have been obtained in the quenched approximation, and one anticipates a refinement of these results as lattice methods continue to advance. In the absence of definitive lattice calculations—and with an eye toward understanding the mechanisms which govern the scale of nucleon strangeness—a variety of model calculations have been performed. The latter have yielded a wide array of predictions for strangeness matrix elements which vary in both magnitude and sign [30–42]. While one might argue *ad nauseum* about the relative merits of different models, there is no compelling reason to take any particular model calculation as definitive.

In an effort to add some clarity to this situation, we discuss in this paper the implications for nucleon strangeness vector current matrix elements of one of the underlying, approximate symmetries of QCD: chiral symmetry. The use of chiral symmetry, in the guise of chiral perturbation theory (CHPT), has proven highly effective in predicting and interpreting a wide variety of low-energy observables [43,44]. The essential strategy of CHPT is to exploit the approximate

*On leave from the Department of Physics, University of Connecticut, Storrs, CT 06269.

$SU(3)_L \times SU(3)_R$ chiral symmetry of QCD for the three lightest flavors to relate one set of observables to another (accounting for loop effects), or to draw on one set of measured quantities to predict another. This approach has recently been employed to analyze of baryon octet and decuplet magnetic moments [45–47] and the nucleon's isovector charge radius [48]. As we illustrate below, this strategy breaks down in the flavor-singlet channel, rendering CHPT unpredictable for the nucleon's strangeness matrix elements. The reason is that the coefficients of the relevant flavor-singlet operators in the chiral Lagrangian, which contain information on short-distance hadronic effects, cannot be determined from existing measurements by using chiral symmetry. Although the leading, nonanalytic long-distance (loop) contributions are calculable [$\mathcal{O}(\sqrt{m_s})$ for the strangeness magnetic moment and $\mathcal{O}(\ln m_s)$ for the strangeness radius], one has no reason to assume that they are numerically more important than the unknown analytic terms arising at the same or lower order from the chiral Lagrangian. The only rigorous way to determine these unknown analytic contributions is to measure the very quantity one would like to predict: the nucleon's flavor-singlet current matrix element.

Consequently, if one wishes to make any predictions at all, one must invoke additional—and therefore model-dependent—assumptions. We illustrate this next line of defense in three forms: (a) a “resonance saturation” model in which the unknown constants arising in chiral perturbation theory are determined by the t -channel exchange of vector mesons; (b) a class of models in which the nucleon's “kaon cloud” is assumed to dominate the strangeness form factors; and (c) constituent chiral quark models in which nucleon's strangeness matrix elements arise from the strangeness content of the constituent U and D quarks. For each of these approaches, we present new calculations and compare them with calculations discussed elsewhere in the literature. The corresponding results are unabashedly model dependent and, therefore, not strong. We give them mainly to illustrate the outer limits to which one might go in employing chiral symmetry to compute $G_E^{(s)}$ and $G_M^{(s)}$. Although there exist additional chiral model approaches not considered in detail here, we believe that the three which we discuss are sufficiently representative so as to illustrate the breadth of predictions permitted by chiral symmetry.

In the end, we argue that each chiral model is plagued by potentially significant uncertainties and fails to include physics which could contribute appreciably to the strangeness form factors. In short, chiral symmetry is only one of several considerations one must factor into an analysis of $G_E^{(s)}$ and $G_M^{(s)}$, and of these considerations, it is not necessarily even the most important. On the other hand, identifying the shortcomings of various chiral models does allow one to see more clearly the elements which should be included in a more credible treatment of the strangeness form factors using effective hadronic methods. An approach incorporating these elements is discussed elsewhere [49].

We organize our discussion of these points as follows. In Sec. II we review the effective low-energy chiral Lagrangians which describe the interaction of pseudoscalar mesons with baryons or quarks. In Sec. III we employ this formalism to compute the nucleon's strange-quark vector

current form factors, introducing model assumptions as necessary. Section IV gives the results of these calculations and a discussion of their credibility. Section V summarizes our conclusions.

II. CHIRAL LAGRANGIANS

In the low-energy world of three-flavor QCD, the QCD Lagrangian manifests an approximate $SU(3)_L \times SU(3)_R$ chiral symmetry. This symmetry is explicitly broken by the small current quark masses. In addition, spontaneous symmetry-breaking $SU(3)_L \times SU(3)_R \rightarrow SU(3)_V$ implies the existence of eight massless (assuming $m_q=0$) Goldstone modes and an axial vector condensate. One identifies the latter with the pion decay constant $f_\pi \approx 93$ MeV and the former with the lowest-lying octet of pseudoscalar mesons. The Goldstone bosons are conveniently described by a field Σ , given by

$$\Sigma = \exp[2i\tilde{\Pi}/f], \quad (1)$$

where $f \equiv f_\pi$ and

$$\tilde{\Pi} = \frac{1}{2} \sum_{a=1}^8 \lambda_a \phi_a, \quad (2)$$

with the λ_a being the eight Gell-Mann matrices and the ϕ_a being the pseudoscalar meson fields [50,51]. The Lagrangian which describes the pseudoscalar kinetic energies and self-interactions is given by

$$\mathcal{L} = \frac{f^2}{4} \text{Tr}(\partial^\mu \Sigma^\dagger \partial_\mu \Sigma) + \frac{f^2}{2} [\text{Tr}(\Sigma \mu M) + \text{H.c.}], \quad (3)$$

where $M = \text{diag}[m_u, m_d, m_s]$ is just the QCD current quark mass matrix which explicitly breaks the residual $SU(3)_V$ symmetry and μ is a parameter which relates the quark masses to quadratic forms in the pseudoscalar masses (hence, $m_{\pi,K}$ is of order $\sqrt{m_q}$). The Lagrangian in Eq. (3) actually constitutes the leading term in an expansion in powers of p/Λ_χ and $\mu M/\Lambda_\chi$, where p denotes the momentum of a low-energy pseudoscalar meson and $\Lambda_\chi \approx 4\pi f \approx 1$ GeV is the scale of chiral symmetry breaking. For purposes of the present study, retention of higher-order terms in the chiral expansion of the purely mesonic sector is not necessary.

Interactions between the Goldstone bosons and matter fields are conveniently described by first introducing vector and axial vector currents

$$V_\mu \equiv \frac{1}{2} (\xi^\dagger \partial_\mu \xi + \xi \partial_\mu \xi^\dagger), \quad (4)$$

$$A_\mu \equiv \frac{i}{2} (\xi^\dagger \partial_\mu \xi - \xi \partial_\mu \xi^\dagger), \quad (5)$$

where $\Sigma = \xi^2$. One may now proceed to construct a chiral Lagrangian for fermions. The simplest case involves the effective, constituent quarks of the quark model. Letting

$$\psi = \begin{pmatrix} U \\ D \\ S \end{pmatrix} \quad (6)$$

denote the triplet of light-quark fields, one has for the leading term in the chiral expansion

$$\mathcal{L}_Q = \bar{\psi}(i\mathcal{D} - m)\psi + g_A \bar{\psi} \mathbf{A} \gamma_5 \psi, \quad (7)$$

where

$$D_\mu \equiv \partial_\mu + V_\mu \quad (8)$$

is a chiral covariant derivative and g_A is a constant which governs the strength of the interaction between quarks and odd numbers of pseudoscalar mesons [the last term in Eq. (7)]. The term involving m gives the constituent quark masses¹ in the limit of good $SU(3)_V$ symmetry. Higher-order terms in the chiral expansion include those which break the degeneracy between the constituent quarks. In the chiral quark model calculation we discuss below, we allow for mass splittings among the constituent quarks, although we will not show the $SU(3)_V$ symmetry-breaking terms explicitly. The higher order terms in the chiral expansion relevant to strangeness vector current matrix elements will be introduced below.

In the case of meson-baryon interactions, we restrict our attention to the lowest-lying octet of baryons, for which one has the matrix representation

$$B \equiv \frac{1}{\sqrt{2}} \sum_{a=1}^8 \lambda_a \psi_a, \quad (9)$$

where the ψ_a are the octet baryon fields. We adopt here the heavy baryon formalism of [23], which avoids problematic terms in the expansion of the baryon chiral Lagrangian involving powers of m_B/Λ_χ , where m_B is the baryon mass. In this formalism, one employs baryon states of good velocity, $v_\mu = p_\mu/m_B$. The corresponding fields are given by

$$B_v(x) \equiv \exp(im_B \not{v} \cdot x) B(x). \quad (10)$$

With this definition, the leading-order heavy baryon chiral Lagrangian is

$$\begin{aligned} \mathcal{L}_v = & i \text{Tr}(\bar{B}_v v \cdot D B_v) + 2D \text{Tr}(\bar{B}_v S_v^\mu \{A_\mu, B_v\}) \\ & + 2F \text{Tr}(\bar{B}_v S_v^\mu [A_\mu, B_v]), \end{aligned} \quad (11)$$

where S_v^λ is a spin operator whose properties are discussed in Ref. [23], where the action of the chiral covariant derivative on the heavy baryon fields is given by

$$D^\mu B = \partial^\mu B + [V^\mu, B], \quad (12)$$

and where D and F are the usual $SU(3)$ reduced matrix elements. The first corrections to \mathcal{L}_v involve one or more powers of quantities which are small in comparison to Λ_χ . For

future reference, we also give the ‘‘traditional’’ nonlinear meson-baryon chiral Lagrangian, which we draw upon in Sec. III B:

$$\begin{aligned} \mathcal{L}_B = & \text{Tr}[\bar{B}(i\mathcal{D} - m_B)B] + D \text{Tr}(\bar{B} \gamma_\mu \gamma_5 \{A^\mu, B\}) \\ & + F \text{Tr}(\bar{B} \gamma_\mu \gamma_5 [A^\mu, B]). \end{aligned} \quad (13)$$

In what follows, we compute strange-quark vector currents of nonstrange chiral quarks and nonstrange baryons arising from kaon loops. To that end, it is useful to work with the baryon number current J_μ^B and to introduce a vector current source Z^μ which couples to J_μ^B via the minimal substitution $\partial^\mu \rightarrow \partial^\mu + i\hat{Q}_B Z^\mu$, where \hat{Q}_B is the baryon number operator.² Taking the first functional derivative with respect to Z^μ of the generating functional yields n -point functions with a single J_μ^B insertion. The strange-quark current is related in a straightforward manner to J_μ^B and the isoscalar EM current [see Eqs. (18)–(22) below]. In practice, it is simpler to compute the strangeness charge of each particle appearing in a Feynman diagram, insert the appropriate Lorentz structure for a vector current, and evaluate the resulting contribution to the strangeness matrix element. From a formal standpoint, however, the use of the baryon number current and of the source Z^μ provides an efficient means for keeping track of the flavor content and chiral order associated with higher moments (mean square radius, magnetic moment, etc.) of various currents.

III. STRANGE-QUARK MATRIX ELEMENTS

With the formalism of Sec. II in hand, it is straightforward to compute nucleon matrix elements of the strange-quark vector current, $\langle p' | \bar{s} \gamma_\mu s | p \rangle$. This matrix element can be parametrized in terms of two form factors, $F_1^{(s)}$ and $F_2^{(s)}$:

$$\langle p' | \bar{s} \gamma_\mu s | p \rangle = \bar{u}(p') \left[F_1^{(s)} \gamma_\mu + i \frac{F_2^{(s)}}{2m_N} \sigma_{\mu\nu} Q^\nu \right] u(p), \quad (14)$$

where $u(p)$ denotes a nucleon spinor and $Q = p' - p$ is the momentum transfer to the nucleon. When working in the heavy baryon formalism, the corresponding Lorentz structures are obtained from Eq. (14) by the use of the relations in Ref. [23]. For on-shell nucleons, the form factors are functions of $Q^2 = q_0^2 - |\vec{q}|^2$, where $Q^\mu = (q_0, \vec{q})$. In what follows, we work with the so-called Sachs electric and magnetic form factors [52], defined as

$$G_E^{(s)} = F_1^{(s)} - \tau F_2^{(s)}, \quad (15)$$

$$G_M^{(s)} = F_1^{(s)} + F_2^{(s)}, \quad (16)$$

where $\tau \equiv -Q^2/4m_N^2$. At $Q^2 = 0$, the Sachs electric form factor gives the net strangeness of the nucleon, which is zero. At small momentum transfer, the scale of this form factor is

²The full chiral structure of the charge operator is given in Ref. [45]. For the present purpose, the inclusion of the full structure is not necessary.

¹Not to be confused with the current quark mass matrix M .

governed by the first derivative with respect to Q^2 , which defines the mean square ‘‘strangeness radius.’’ We work with a dimensionless version of this quantity, ρ_S^s , defined as

$$\rho_S^s = \left. \frac{dG_E^{(s)}}{d\tau} \right|_{\tau=0} = -\frac{2}{3} m_N^2 \langle r_s^2 \rangle^S, \quad (17)$$

where $\langle r_s^2 \rangle^S$ is the dimensionful Sachs strangeness radius and where the superscript ‘‘S’’ denotes the Sachs, as distinct from the Dirac, radius. There exists no symmetry principle which constrains the strangeness magnetic moment, $G_M^{(s)}(0) = \mu^s$. Note that since $G_E^{(s)}(0) = 0$ one has $\mu^s = \kappa^s$. In discussing the implications of chiral symmetry for $\langle p' | \bar{s} \gamma_{\mu} s | p \rangle$, we will be concerned primarily with these two parameters, ρ^s and μ^s .

A. Heavy baryon chiral perturbation theory

In terms of chiral counting, the strangeness magnetic moment and radius, like the corresponding electromagnetic quantities, appear, respectively, as order $1/\Lambda_\chi$ and $1/\Lambda_\chi^2$ corrections to the leading-order heavy baryon Lagrangian given in Eq. (11). In discussing these corrections, it is convenient to rewrite the strangeness vector current in terms of the electromagnetic and baryon number currents:

$$J_\mu^{\text{EM}}(T=1) = V_\mu^{(3)}, \quad (18)$$

$$J_\mu^{\text{EM}}(T=0) = (1/\sqrt{3}) V_\mu^{(8)}, \quad (19)$$

$$J_\mu^B = V_\mu^{(0)}, \quad (20)$$

where the $T=1$ and $T=0$ designations indicate the isovector and isoscalar electromagnetic currents, where ‘‘B’’ denotes the baryon number current, and where

$$V_\mu^{(a)} = \frac{\lambda^a}{2} \gamma_{\mu} q, \quad q = \begin{pmatrix} u \\ d \\ s \end{pmatrix}. \quad (21)$$

Here, the $\lambda^a, a=1, \dots, 8$ are the usual Gell-Mann matrices, $\lambda^0 = \frac{2}{3} \mathbf{1}$, and q gives the triplet of QCD quark fields. In terms of the currents in Eqs. (18)–(20) one has

$$\bar{s} \gamma_{\mu} s = J_\mu^B - 2J_\mu^{\text{EM}}(T=0). \quad (22)$$

With these definitions one may write down the higher-order heavy baryon Lagrangians corresponding to the EM and baryon number magnetic moments and charge radii:

$$\begin{aligned} \Delta \mathcal{L}_{\text{EM}}^{T=1} &= \frac{e}{\Lambda_\chi} \epsilon_{\mu\nu\alpha\beta} v^\alpha \{ b_+ \text{Tr}(\bar{B}_\nu S_\nu^\beta \{\lambda^3, B_\nu\}) \\ &\quad + b_- \text{Tr}(\bar{B}_\nu S_\nu^\beta [\lambda^3, B_\nu]) \} F^{\mu\nu} \\ &\quad - \frac{e}{\Lambda_\chi^2} \{ c_+ \text{Tr}(\bar{B}_\nu \{\lambda^3, B_\nu\}) \\ &\quad + c_- \text{Tr}(\bar{B}_\nu [\lambda^3, B_\nu]) \} v_\mu \partial_\lambda F^{\mu\lambda}, \end{aligned} \quad (23)$$

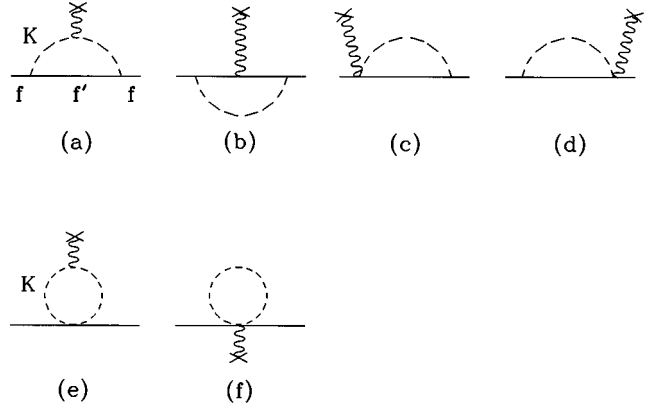


FIG. 1. One kaon loop contributions to strangeness vector current form factors of a nonstrange fermion f (nucleon or constituent quark). Here, \times denotes insertion of the current $\bar{s} \gamma_{\mu} s$ and f' denotes a strangeness +1 fermion (e.g., Λ or constituent S quark).

$$\begin{aligned} \Delta \mathcal{L}_{\text{EM}}^{T=0} &= \frac{e}{\Lambda_\chi} \frac{1}{\sqrt{3}} \epsilon_{\mu\nu\alpha\beta} v^\alpha \{ b_+ \text{Tr}(\bar{B}_\nu S_\nu^\beta \{\lambda^8, B_\nu\}) \\ &\quad + b_- \text{Tr}(\bar{B}_\nu S_\nu^\beta [\lambda^8, B_\nu]) \} F^{\mu\nu} \\ &\quad - \frac{e}{\Lambda_\chi^2} \frac{1}{\sqrt{3}} \{ c_+ \text{Tr}(\bar{B}_\nu \{\lambda^8, B_\nu\}) \\ &\quad + c_- \text{Tr}(\bar{B}_\nu [\lambda^8, B_\nu]) \} v_\mu \partial_\lambda F^{\mu\lambda}, \end{aligned} \quad (24)$$

$$\begin{aligned} \Delta \mathcal{L}_B &= \frac{b_0}{\Lambda_\chi} \epsilon_{\mu\nu\alpha\beta} v^\alpha \text{Tr}(\bar{B}_\nu S_\nu^\beta B_\nu) Z^{\mu\nu} \\ &\quad - \frac{c_0}{\Lambda_\chi^2} \text{Tr}(\bar{B}_\nu B_\nu) v_\mu \partial_\lambda Z^{\mu\lambda}, \end{aligned} \quad (25)$$

where $F^{\mu\nu}$ is just the ordinary EM field strength tensor, $Z^{\mu\nu}$ is the analogous quantity involving the source Z^μ coupling to baryon number, and e is the proton's EM charge. In each $\Delta \mathcal{L}$, the terms of order $1/\Lambda_\chi$ contribute to the anomalous magnetic moment and those of order $1/\Lambda_\chi^2$ enter the charge radius [53]. For a given baryon, the magnetic moment and mean square radius will contain a contribution from $\Delta \mathcal{L}$ and a contribution from loops (nonanalytic in m_q), as in Fig. 1:

$$\kappa^a = \kappa_{\text{loop}}^a + \left(\frac{2m_B}{\Lambda_\chi} \right) b^a, \quad (26)$$

$$\rho_D^a = \rho_{\text{loop}}^a - \left(\frac{2m_B}{\Lambda_\chi} \right)^2 c^a, \quad (27)$$

where $\kappa^a = F_2^{(a)}(0)$ is the anomalous magnetic moment, ‘‘a’’ denotes the corresponding flavor channel [$T=0,1, s$, SU(3) singlet], and the subscript ‘‘D’’ indicates the slope of the Dirac form factor (F_1) at $\tau=0$. In the case of the EM moments, the quantities b^a and c^a contain appropriate linear combinations of b_\pm and c_\pm as determined from the traces appearing in Eqs. (23)–(24). Using the heavy baryon formal-

ism outlined above, we compute κ_{loop}^a and ρ_{loop}^a employing dimensional regularization. For the strangeness moments, we find

$$\kappa_{\text{loop}}^s = (2\pi) \left[\left(\frac{3F+D}{\sqrt{6}} \right)^2 + \frac{3}{2}(D-F)^2 \right] \frac{m_N}{\Lambda_\chi} \frac{m_K}{\Lambda_\chi}, \quad (28)$$

$$\rho_{\text{loop}}^s = \left(\frac{m_N}{\Lambda_\chi} \right)^2 \left\{ 1 + \frac{5}{3} \left[\left(\frac{3F+D}{\sqrt{6}} \right)^2 + \frac{3}{2}(D-F)^2 \right] \right\} \times \left[C_\infty - \ln \frac{m_K^2}{\mu^2} \right], \quad (29)$$

where $C_\infty = 1/\varepsilon - \gamma + \ln 4\pi$ with $\varepsilon = (4-d)/2$ and d being the number of dimensions. One finds analogous expressions for the isovector (λ^3) and isoscalar ($\lambda^8/\sqrt{3}$) components of the EM moments [45,54]. The constant c^s appearing in Eq. (27) contains the appropriate dependence on C_∞ to cancel the pole term in ρ_{loop}^s . The scale μ denotes the scale at which the subtraction of the pole term is carried out. The remaining finite parts of $(\kappa_{\text{loop}}^s, \rho_{\text{loop}}^s)$ and of (b^s, c^s) determine the value of the anomalous magnetic moment and mean square Dirac radius. Using Eqs. (22)–(25), one can express the ‘‘low-energy’’ constants (b^s, c^s) in terms of the corresponding quantities for the baryon and EM currents:³

$$b^s = b_0 - 2[b_- - (b_+/3)], \quad (30)$$

$$c^s = c_0 - 2[c_- - (c_+/3)]. \quad (31)$$

In the case of the EM moments, the (b_\pm, c_\pm) are fit to known EM moments in the baryon octet. One may then employ Eqs. (23)–(27) and the loop contributions to predict the moments of other baryons within the octet. This approach reflects the basic strategy of chiral perturbation theory: rely on chiral symmetry to relate one set of quantities (known EM moments) to another (those one wishes to predict), modulo loop corrections (a consequence of spontaneous chiral symmetry breaking). A simple fit to the nucleon EM moments alone gives $b_+ \approx 1.4$, $b_- \approx 0.9$, $c_+ \approx -1.9$, $c_- \approx 0.9$ [55].

As one would expect on general grounds, these constants are of order unity. In the case of the nucleon EM anomalous magnetic moments, the contributions from the b_\pm and the loops have comparable magnitudes. In the case of the charge radii, the loops give the dominant contribution to the isovector EM charge radius while the c_\pm give the dominant contribution to the isoscalar EM charge radius. It is evident, then, that one cannot rely on either the loop or the ‘‘counterterm’’ contributions alone to account for the nucleon’s EM moments.

In the case of the strangeness magnetic moment and radius, one would ideally follow a similar strategy. However, the coefficients b^s and c^s are unknown. The reason is that these constants depend on b_0 and c_0 as well as the b_\pm and c_\pm . Since the baryon number magnetic moment and charge

radius for the octet baryons have not been measured, b_0 and c_0 are undetermined. In fact, by virtue of Eq. (22), measurements of the strangeness radius and magnetic moment of the nucleon would provide a determination of the corresponding quantities for the baryon number current and, through Eqs. (30) and (31), would fix b_0 and c_0 . Moreover, given the situation in the EM case, one would not be safe in assuming that b^s and c^s differ significantly in magnitude from unity. Indeed, one has no reason to expect, based on any symmetry principle, that either the loops or chiral counterterms should give the dominant contributions to the strangeness radius and magnetic moment. Thus, chiral perturbation theory, in its purest form, cannot make a prediction for the strangeness vector current matrix elements.

In arriving at this conclusion, we did not include decuplet baryons in the loops nor the subleading nonanalytic loop contributions ($\sqrt{m_s} \ln m_s$ in the case of the strangeness magnetic moment) as was done in Ref. [45]. In that work, it was found that the dominant loop contribution to the magnetic moments is $\mathcal{O}(\sqrt{m_s})$ and that the inclusion of the decuplet states does not have the same kind of effect as it does in the axial vector matrix elements, where non-negligible octet-decuplet cancellations occur for the loop contributions. Similarly, we did not use the one-loop corrected axial meson-nucleon couplings. Although from a formal standpoint the difference between tree-level and one-loop corrected couplings is of higher order than we are considering here, the authors of Ref. [45] obtained a better fit to the baryon magnetic moments with the corrected couplings. The use of the latter effectively reduces the size of the large kaon loop contributions. As we note below, the physics which modifies one-loop results largely amounts to kaon rescattering (see, e.g., Ref. [56]). Employing one-loop corrected axial couplings in the one-loop magnetic moment calculation incorporates some, but not all, rescattering contributions. It is not entirely clear that the impact of two-loop contributions to the magnetic moment is numerically less significant than the replacement of tree-level with one-loop corrected axial couplings in the one-loop magnetic moment calculation. In the present instance, we avoid this issue altogether and restrict our attention to one-loop effects.

B. Chiral models

The conclusion of the foregoing analysis implies that in order to make predictions for the nucleon’s strangeness moments, one must go beyond the framework of CHPT and invoke additional, model dependent assumptions. To this end, a number of possibilities present themselves. We consider three such model approaches: (a) resonance saturation, (b) kaon cloud dominance, and (c) constituent chiral quarks. These approaches range from one remaining close to the framework of CHPT by estimating the chiral counterterms [model (a)] to an attempt to apply chiral symmetry on the microscopic level [model (c)].

Resonance saturation. One might attempt to estimate the chiral counterterms b^s and c^s , for example, by assuming that the corresponding terms in $\Delta\mathcal{L}$ arise from t -channel vector meson exchanges. The rationale for such an approach derives primarily from one’s experience in the purely mesonic sector where, at $\mathcal{O}(p^4)$ in the chiral expansion, one encounters ten

³Henceforth, the cancellation of the C_∞ will be understood and (b^a, c^a) will denote the finite remainders of the counterterms.

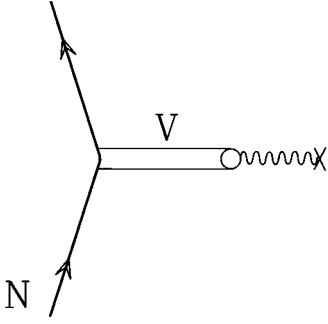


FIG. 2. Resonance contribution to nucleon vector current form factors. Here V denotes a vector meson and \times denotes a vector current (EM, strangeness, baryon number, etc.).

scale-dependent counterterms, $L_i^r(\mu)$ [57,58]. Five of these counterterms ($i=1,2,3,9,10$) agree quite well with the predictions of vector meson exchange when the renormalization scale is chosen to be $\mu \approx m_\rho$. Of particular interest is the pion EM charge radius, which receives a contribution from $L_9^r(\mu)$. This counterterm contribution dominates $\langle r_\pi^2 \rangle$, with the one-loop contribution giving roughly 7% of the total (for $\mu = m_\rho$). Were this situation to carry over into the arena of the nucleon's vector current form factors, one would then expect the counterterms b^a and c^a to be given by vector meson resonances, as shown in Fig. 2.

To explore this possibility further, one requires the couplings of $J^{PC}=1^{--}$ vector mesons V to spin-1/2 baryons and to electroweak vector bosons. Although it is conventional to describe the vector mesons by a vector field V_μ , we choose instead to follow Refs. [57,58] and work with a formulation in terms of a two-index antisymmetric tensor, $V_{\mu\nu}$. This formulation offers the advantages that (a) it is straightforward to write down a gauge-invariant Lagrangian for the interaction of the vector meson with electroweak vector bosons, and (b) the contributions from the diagram in Fig. 2 do not affect the normalization of the Dirac form factor at $Q^2=0$. In addition, one finds, as shown in Ref. [57], that the vector field formulation does not generate a vector meson contribution to the pion EM charge radius—a situation one must remedy by the introduction of an additional term at $\mathcal{O}(p^4)$ in the chiral Lagrangian. No such term is necessary with the tensor formulation. The primary cost involved in using the antisymmetric tensor formulation is the presence of a four-index vector meson propagator. For the calculation of tree-level process such as given in Fig. 2, this cost is not exorbitant. Since the details of this formulation and its relation to the vector field framework are discussed in Refs. [57,58], we refer the reader to those papers and simply give the form of the couplings and results for the nucleon form factors.

The vector meson contributions to the nucleon magnetic moment and charge radius are generated by the following VNN effective Lagrangian:

$$\mathcal{L}_{VNN} = 2G_T \epsilon^{\mu\nu\alpha\beta} V_\alpha \bar{B}_\nu S_\beta^v B_\nu V_{\mu\nu} + \frac{G_V}{\Lambda_\chi} \bar{B}_\nu B_\nu v_\mu D_\nu V^{\mu\nu}, \quad (32)$$

while the gauge-invariant coupling vector meson-photon coupling is given by

$$\mathcal{L}_{V\gamma} = \frac{eF_V\Lambda_\chi}{\sqrt{2}} V_{\mu\nu} F^{\mu\nu}. \quad (33)$$

A similar expression applies to the coupling of V and Z (the source of the baryon number current). We have omitted SU(3) indices for simplicity. In the formalism of Refs. [57,58], the field $V_{\mu\nu}$ has dimension 1. The factors of Λ_χ have been introduced to maintain the correct dimensionality while employing dimensionless couplings. In this respect, our definition of F_V differs from that of Refs. [57,58], where the corresponding coupling has mass dimensions. The values for the F_V can be extracted from the rates $\Gamma(V \rightarrow e^+ e^-)$. In the case of the lightest isovector vector meson, for example, one has $F_\rho = 0.132$. (The relation between the constants G_V , G_T , and F_V and those used in the vector field formulation [59–63] is obtained in a straightforward manner.)

From these couplings and the amplitude associated with the diagram of Fig. 2, we find the following contributions to the Dirac and Pauli form factors from a single vector meson:

$$F_1(Q^2) = \sqrt{2} G_V F_V \frac{Q^2}{m_V^2 - Q^2}, \quad (34)$$

$$F_2(Q^2) = 4\sqrt{2} G_T F_V \frac{m_N \Lambda_\chi}{m_V^2} \frac{m_V^2}{m_V^2 - Q^2}, \quad (35)$$

where m_V is the vector meson mass. Note that $F_1(Q^2=0) = 0$, so that the vector meson resonances do not affect the nucleon charge.

From Eqs. (34)–(35), one can extract the vector meson contributions to the nucleon magnetic moment and charge radius and, thus, the corresponding contributions to the chiral coefficients b and c :

$$b = 2\sqrt{2} G_T F_V \left(\frac{\Lambda_\chi}{m_V} \right)^2, \quad (36)$$

$$c = \sqrt{2} G_V F_V \left(\frac{\Lambda_\chi}{m_V} \right)^2, \quad (37)$$

where the flavor index “ a ” has been omitted for simplicity. In the case of the nucleon's EM form factors, the expressions in Eqs. (36) and (37), together with the decay rates for $V \rightarrow e^+ e^-$, can be used to determine the couplings G_V , G_T , and F_V [61–63]. Were one also to possess knowledge of the F_V associated with the strangeness matrix elements $\langle 0 | \bar{s} \gamma_\mu s | V \rangle$, one could then use the expressions in Eqs. (36) and (37) to derive the counterterms for the nucleon's strangeness form factors. However, one does not at present possess such knowledge. As a fallback strategy, one may invoke one's knowledge of the flavor content of the vector meson wave functions, where such knowledge exists. In doing so, it is useful to follow the spirit of Refs. [30,61,62] and write down dispersion relations for the nucleon form factors:

$$F_1^{(a)}(Q^2) - F_1^{(a)}(0) = Q^2 \sum_V \frac{a_V^{(a)}}{m_V^2 - Q^2} + Q^2 \tilde{f}_1^{(a)}(Q^2), \quad (38)$$

$$F_2^{(a)}(Q^2) = \sum_V \frac{m_V^2 b_V^{(a)}}{m_V^2 - Q^2} + \tilde{f}_2^{(a)}(Q^2), \quad (39)$$

where the superscript (a) denotes the flavor channel ($T=0,1$ or strangeness), where the poles arise from vector meson exchange as in Fig. 2, and where the functions $f_i(Q^2)$ represent contributions from the multimeson continuum.⁴ In the works of Refs. [30,61,62], the continuum contributions were neglected in the isoscalar and strangeness channels. In the spirit of resonance saturation, we retain the leading, nonanalytic loop contributions as an estimate of the continuum terms and assume that the counterterms b^a and c^a are dominated by the vector meson pole contributions. From Eqs. (34)–(39), these counterterms are easily related to the pole residues:

$$b^a = \left(\frac{\Lambda_\chi}{2m_N} \right) \sum_V b_V^{(a)}, \quad (40)$$

$$c^a = \sum_V a_V^{(a)} \left(\frac{\Lambda_\chi}{m_V} \right)^2. \quad (41)$$

Thus, for purposes of determining the chiral coefficients b^a and c^a , it is just as effective to work with the residues in a pole analysis of the form factors as it is to try and determine the hadronic couplings G_V , G_T , and F_V .

A determination of the residues was carried out by the authors of Refs. [61,62], who employed a three-pole fit to the isoscalar EM form factors. The poles were identified, respectively, with the ω , ϕ , and one higher mass isoscalar vector meson V' (for an update, see Ref. [64]). The inclusion of at least two poles was needed in order to reproduce the observed dipole behavior of the isoscalar form factors. The authors found that a third pole was needed in order to obtain an acceptable χ^2 for the fit. Subsequently, Jaffe [30] observed that since the physical ω and ϕ are nearly pure $u\bar{u} + d\bar{d}$ and $s\bar{s}$ states, respectively, one can relate the residues appearing in the strangeness form factor dispersion relations to those associated with the isoscalar EM form factors:

$$\begin{aligned} \frac{a_\omega^s}{a_\omega^{T=0}} &= -\sqrt{6} \left[\frac{\sin \epsilon}{\sin(\epsilon + \theta_0)} \right], \\ \frac{a_\phi^s}{a_\phi^{T=0}} &= -\sqrt{6} \left[\frac{\cos \epsilon}{\cos(\epsilon + \theta_0)} \right], \end{aligned} \quad (42)$$

where ϵ is the mixing angle between the pure $u\bar{u} + d\bar{d}$ and pure $s\bar{s}$ states and θ_0 is the ‘‘magic’’ octet-singlet mixing angle giving rise to these pure states. Analogous formulas apply for the residues appearing in the expressions for $F_2^{(s)}$. From Eqs. (40)–(42), one may now determine the ω and ϕ contributions to the constants b^s and c^s .

A determination of the remaining residues $a_{V'}^s$ and $b_{V'}^s$ is more problematic. One does not possess sufficient knowledge of the V' flavor content to derive a simple relation

TABLE I. Theoretical predictions for nucleon strange quark vector current form factors. Columns two and three give dimensionless mean square Dirac strangeness radius and strangeness anomalous magnetic moment, respectively. The fourth column gives the Sachs strangeness radius: $\rho_s^s = \rho_D^s - \mu^s$. To convert to $\langle r_s^2 \rangle$, multiply ρ^s by -0.066 fm^2 . The first three lines give predictions of chiral models discussed in this work: (a) heavy baryon CHPT/resonance saturation employing ω and ϕ residues of fit. 8.2 of Ref. [62]; numbers in parentheses give leading, nonanalytic (in m_s) loop contributions for $\mu = m_\omega$; (b) nonlinear σ model with hadronic form factors using cutoff mass $\Lambda = 1.2 \text{ GeV}$; (c) chiral quark model with cutoff mass $\Lambda = 1.0 \text{ GeV}$, oscillator parameter $\gamma = 1.93 \text{ fm}^{-1}$, and $m_U = m_D = 0.33 \text{ GeV}$. Last four lines give previously reported predictions: (d) three pole model of Ref. [30]; (e) linear σ model of Ref. [31]; (f) hybrid pole/loop model of Ref. [34]; (g) cloudy bag model of Ref. [32].

Model	ρ_D^s	μ^s	ρ_s^s
Resonance sat. ^(a)	$-3.62(1.52)$	$1.85(2.2)$	$-5.47(-0.68)$
NL Σ M/FF ^(b)	0.11	-0.25	0.36
Chiral quarks ^(c)	0.53	-0.09	0.62
Poles ^(d)	-2.43 ± 1.0	-0.31 ± 0.009	-2.12 ± 1.0
L Σ M/FF ^(e)	0.1	$-(0.31-0.40)$	$0.41-0.49$
Hybrid ^(f)	0.37	$-(0.24-0.32)$	$0.61-0.68$
CBM ^(g)	0.15	-0.09	0.24

between the strangeness and isoscalar EM residues. One must therefore employ alternative strategies. Jaffe arrived at values for the $a_{V'}^s$ and $b_{V'}^s$ by imposing conditions on the asymptotic behavior of the form factors ($Q^2 \rightarrow \infty$). Using a three-pole fit, with all masses and two residues fixed, one is only able to require that $F_1^{(s)}$ vanish as $1/Q^2$ and $F_2^{(s)}$ as $(1/Q^2)^2$. These asymptotic conditions are more gentle than one would expect based on the most naïve quark counting rules. As discussed in Refs. [40,41], consistency with the latter would require the inclusion of more poles with unknown masses and residues than used in the fits of Refs. [30,61,62,64]. Since the adequacy of these quark counting rules for strangeness form factors is itself not clear, and since one’s predictions for the nucleon’s strangeness radius and magnetic moment within this framework are nontrivially dependent on one’s assumptions about asymptopia [40,41], this approach to treating the V' contribution is ambiguous at best.

Another alternative is to note that in the fits of Ref. [62], the V' contributes very little to the isoscalar mean square radius and anomalous magnetic moment (less than 10% in the fits with the best χ^2). Indeed, the primary benefit of including the V' was to obtain acceptable χ^2 over the full range of Q^2 used in the fit; its impact on the value of the form factors and their slopes at the origin is minimal. The latter result is not surprising, since (a) it is necessary to include only the two lightest poles in order to reproduce the observed dipole behavior of the isoscalar form factor, and (b) the V' contribution to the low- $|Q^2|$ behavior of the form factors is suppressed by powers of $(m_{\omega,\phi}/m_{V'})^2$ relative to the ω and ϕ contributions. Using analogous logic, it might seem reasonable to neglect the V' when seeking to determine the leading, nontrivial Q^2 behavior of the strangeness form factors. In Table I, we quote results for the nucleon’s Dirac

⁴Note that the continuum contribution need not enter additively; one may also include it as a multiplicative factor [63,64]. We write it additively for simplicity of illustration.

strangeness radius and magnetic moment assuming the ω and ϕ residues saturate the constants b^s and c^s . We obtain these constants using the Jaffe relations in Eq. (42), the results from fit 8.2 of Ref. [62] (which gives the best χ^2)⁵, and Eqs. (40) and (41).

We expect this approach to yield a rough upper bound on the resonance saturation predictions for $|b^s|$ and $|c^s|$. Indeed, if the asymptotic behavior of the strangeness form factors follows that of the isoscalar EM form factors, then the two lightest poles ought to give the dominant resonance contributions to the leading moments, as in the isoscalar case. If, however, the strangeness form factors fall off more rapidly than $(1/Q^2)^2$ at large momentum transfer, the presence of higher mass poles might be required to cancel the leading high- Q^2 behavior arising from the ω and ϕ pole contributions. In this case, contributions from the V' (or beyond) to the leading strangeness moments would reduce the combined ω and ϕ contribution [40,41], thereby modifying the values quoted in Table I. One should also note that the presence of higher-mass poles is not absolutely essential for modifying the Q^2 dependence of the form factors. A strong, nonresonant, multimeson continuum contribution could offset the leading large- Q^2 behavior generated by the lightest poles. Given these ambiguities, then, we take the two-pole resonance saturation predictions as crude estimates of the magnitudes which b^s and c^s might attain in this approach.

Kaon cloud dominance. A second possibility is to relax the requirement that one undertake a consistent chiral expansion and use kaon loops alone to make a prediction. The rationale for this approach has a twofold basis. The first follows from a geometric interpretation of the nucleon charge radius, wherein it characterizes a spatial asymmetry in the charge distribution. In this picture, a spatial polarization of the strange sea arises from fluctuations of the nucleon into a kaon and strange baryon. The kaon, having about half the mass of the lightest strange baryons lives on average further from the nucleon center of mass than the strange baryon. One would expect, then, to obtain a negative value for $\langle r_s^2 \rangle$ (positive value for ρ^s), since the kaon carries the \bar{s} . Implicit in this picture is an assumption that $s\bar{s}$ pair creation by the neutral gauge boson probe, which also contributes to the Dirac or electric form factors and which appears partially in the guise of resonance contributions, is negligible compared to the mechanism of $s\bar{s}$ spatial polarization. The kaon cloud dominance approach also assumes that the multipion contribution is negligible when compared to that of the kaon cloud, ostensibly because the pion contains no valence s or \bar{s} quarks.

The second motivation draws on the result of a pion loop calculation of the nucleon's EM form factors carried out by Bethe and DeHoffman [65]. This calculation was performed using the equivalent of the linear σ model. At the time they were reported, the results were in surprising agreement with the experimental values for the nucleon's charge radii and

magnetic moments, despite the large value of the πN coupling which enters this perturbative calculation. The lore which developed in the aftermath of this calculation is that the pion cloud dominates the nucleon's isovector EM moments and that a one-loop calculation sufficiently incorporates the physics of the pion cloud. Were this situation to persist in the strangeness sector, one would expect that the kaon cloud gives the dominant contribution to the ρ^s and μ^s and that a one-loop calculation would suffice to give their correct magnitude and sign.

A variety of one-loop calculations have been performed assuming that the kaon cloud dominates the strange form factors. For example, the authors of Ref. [31] computed ρ_s and μ_s within the context of the SU(3) linear σ model. Within this framework, the leading strangeness moments are UV finite. Nevertheless, the calculation was performed by including hadronic form factors at the $KN\Lambda$ vertices, drawing on results of fits to baryon-baryon scattering in the one meson exchange approximation which find better agreement with data if hadronic form factors are included. The authors of Refs. [33,34] extended this approach to compute both the leading moments as well as the nonleading Q^2 dependence of the strangeness form factors using a hybrid kaon-loop-vector-meson pole model. Although the hybrid model goes beyond a simple one-loop approximation, it nevertheless represents a type of kaon cloud model inasmuch as nonresonant multipion contributions are omitted. Another variation of this general approach is a study performed using the cloudy bag model (CBM) and the "cloudy" constituent quark model (CCQM) [32]. The CBM represents a kind of marriage of the MIT bag model with spontaneously broken chiral symmetry. The strength of the meson-baryon vertices is determined by the meson-quark coupling and the quark's bag model wave function. The CCQM is similar in spirit, though in this case the nonrelativistic constituent quarks are confined with a harmonic oscillator potential. In effect, the CBM and CCQM calculations represent kaon loop calculations in which the $N\Lambda K$ and $N\Sigma K$ form factors are determined by the dynamics of the particular models. More recently, Geiger and Isgur have extended the kaon cloud idea to include one loop contributions from all known strange mesons and baryons using the nonrelativistic quark model to obtain a nucleon-strange hadron vertex function [39].

In all cases, these models include contributions which are both nonanalytic and analytic in the s -quark mass, effectively modeling contributions from the relevant higher-dimension operators appearing in an effective Lagrangian. Moreover, in each instance the loop integration was cutoff at some momentum scale by including form factors at the hadronic vertices. In both respects, a consistent chiral expansion is lost. In principle, higher-order Lagrangians and loops could yield terms of the same chiral order as some of the analytic terms retained from the one-loop amplitudes. Similarly, the use of hadronic form factors with a cutoff parameter breaks the consistency of the expansion because a new scale is introduced (e.g., the 1/hadron size) and/or because the form factor itself contributes like an infinite tower of higher-dimension operators.

One might argue that since m_K/Λ_χ is not small, the chiral expansion is not all that useful in the case of strange quarks and that models inconsistent with this expansion may yet be

⁵The results using the other two fits of Ref. [62] give smaller magnitudes for ρ_D^s and μ^s . Using the updated fit of Ref. [64] (see also Ref. [42]), and a somewhat larger ω - ϕ mixing angle than used in Ref. [30] one obtains a larger Dirac strangeness radius than quoted in Table I.

credible [66,67]. We wish to illustrate, nonetheless, that the approach of kaon cloud dominance still presents a host of uncertainties. To do so, we compute the one-loop contributions to ρ^s and μ^s using the nonlinear SU(3) σ model. Since, in this instance, we are no longer concerned to obtain a convergent chiral expansion, we retain an explicit dependence on the baryon mass and employ the “traditional” Lagrangian of Eq. (13). The relevant diagrams are shown in Fig. 1. The calculation is similar to that of Ref. [31], which was carried out using the linear SU(3) σ model. In the present case, the strangeness radius is UV divergent, unless one includes form factors at the hadronic vertices. A simple choice, and one which renders the loop calculation most tractable, is the monopole form

$$F(k^2) = \frac{m_K^2 - \Lambda^2}{k^2 - \Lambda^2}, \quad (43)$$

where k is the momentum of the kaon appearing at the $KN\Lambda$ vertex and Λ is a momentum cutoff. The monopole

$$\left(\pm i Z_\mu (Q^\mu \pm 2k^\mu) \frac{\{F[(Q \pm k)^2] - F(k^2)\}}{[(Q \pm k)^2 - k^2]} k^\lambda [\hat{Q}, \tilde{\Pi}] + i Z^\lambda F[(Q \pm k)^2] [\hat{Q}, \tilde{\Pi}] \right) \bar{u} \gamma_\lambda \gamma_5 u, \quad (45)$$

where $\tilde{\Pi}$ is the pseudoscalar octet matrix defined in Sec. II, Q_μ is the momentum of the source Z (for EM or baryon number current), \hat{Q} is the corresponding charge, and where the upper (lower) sign corresponds to an incoming (outgoing) meson.

In Sec. IV and Table I we give the results of the kaon loop calculation using the nonlinear SU(3) σ model and hadronic form factors [as in Eq. (43)] as a function of the cutoff Λ . We compare these results with those of other kaon cloud models in order to estimate the range in predictions which arises under the rubric of kaon cloud dominance. Indeed, the existence of such a range reflects the ambiguities associated with this general approach. We discuss these ambiguities further in Sec. IV.

Constituent quarks. The final model approach we consider entails treating the nucleon’s strangeness matrix elements as arising from the strangeness “content” of constituent U and D quarks. The motivation for this approach derives from a picture of the constituent quark as a current quark of QCD surrounded by a sea of gluons and $q\bar{q}$ pairs. It follows that the nucleon’s strangeness radius and magnetic moment arise from the corresponding quantities for the constituent U and D quarks [68].⁶ The procedure one follows within this framework is essentially the quark model analog of the one-body approximation made in computing nuclear current matrix elements [38]. Specifically, one derives an operator associated with the individual constituents (quarks, nucleons) and computes a matrix element of that operator using the

form above was employed in the Bonn potential fits to baryon-baryon scattering, and value of the cut-off $\Lambda \sim 1.2 - 1.4$ GeV was obtained [60]. Various kaon cloud models differ, in part, through the choice of form for $F(k^2)$ and the value of the cutoff parameter.

The inclusion of a hadronic form factor necessitates the introduction of additional, “seagull” graphs in order to maintain the gauge invariance of the calculation [Figs. 1(c) and (d)]. Without these new graphs, the loop calculation with hadronic form factors does not satisfy the vector current Ward-Takahashi identity. It was shown in Refs. [31,33] that use of the minimal substitution $k_\mu \rightarrow k_\mu + i\hat{Q}Z_\mu$ in $F(k^2)$ generates a set of seagull vertices whose loop graphs restore agreement of the calculation with the WT identity. It is straightforward to show that for a meson-nucleon vertex of the form

$$\mp i F(k^2) k^\lambda \tilde{\Pi} \bar{u} \gamma_\lambda \gamma_5 u \quad (44)$$

the corresponding seagull vertex is

appropriate bound state (hadron, nucleus) wave function. Chiral symmetry is invoked in deriving the constituent quark strangeness current operators. Such a calculation of ρ_S^s was performed by the authors of Ref. [33], using the Nambu–Jona-Lasinio (NJL) model [69] to compute the constituent quark strangeness radii.

An alternative is to adopt a chiral quark model framework, wherein the constituent quark strangeness currents arise from fluctuations of the constituent U and D quarks into a kaon plus a constituent S quark. The contributions from the individual U and D quarks are added to give the total nucleon strangeness matrix element using a quark model spin-space-flavor wave function, as illustrated schematically in Fig. 3. The strength of the kaon-constituent quark interaction is governed by the parameter g_A appearing in the chiral Lagrangian of Eq. (7). This parameter can be determined by using the constituent chiral quark model to compute the nucleon’s axial vector current. Since g_A enters

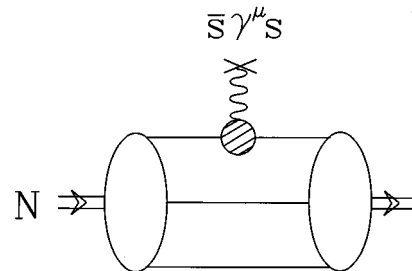


FIG. 3. Chiral quark model for nucleon strangeness. Shaded circle represents strange-quark vector current matrix element of a constituent U or D quark, generated by the processes shown in Fig. 1.

⁶The CCQM calculations of Ref. [32] omit contributions from the strangeness content of the constituent quarks. Only the kaon cloud around the entire bag of quarks is considered.

the strangeness matrix element of the nucleon at one-loop order, one need only determine it at tree level (see below).

It is worth noting that the chiral quark model does not suffer from the same lack of convergence which plagues the traditional baryon chiral Lagrangian [Eq. (13)] due to the size of m_B . Since the constituent quark mass is considerably smaller than Λ_χ , one has reason to believe that higher-order corrections to the leading-order Lagrangian in Eq. (7), as well as higher-order loop effects, will be suppressed. On the other hand, the ambiguity associated with the coefficients b^s and c^s remains. In the case of chiral quarks, one may still write down corrections to \mathcal{L}_Q associated with the magnetic moment and Dirac charge radius of a constituent quark that are, respectively, of lower order and the same order in $1/\Lambda_\chi$ as the corresponding contributions from loops:

$$\Delta\mathcal{L} = \frac{b_q^a}{2\Lambda_\chi} \bar{\psi} \sigma_{\mu\nu} \hat{Q} \psi F^{\mu\nu} - \frac{c_q^a}{\Lambda_\chi^2} \bar{\psi} \gamma_\mu \hat{Q} \psi \partial_\nu F^{\mu\nu}, \quad (46)$$

where \hat{Q} is the appropriate charge (EM or baryon number), $F^{\mu\nu}$ is the field strength associated with the corresponding source, and the ‘‘a’’ superscript denotes the flavor channel [70].

As in the case of the baryon chiral Lagrangian, the coefficients b_q^0 and c_q^0 in the SU(3)-singlet channel cannot be determined from known moments. Consequently, one must invoke additional model assumptions in order to make chiral quark model predictions for the nucleon’s strangeness matrix elements. In the present study, we adopt the following strategy. First, we simply omit the contributions from the b_q^a and c_q^a and take the constituent-quark–kaon one-loop contribution as an indication of the scale of the constituent quark strangeness radius and magnetic moment. Although this assumption, which represents our model ansatz, may appear to be a drastic approximation, it is no more questionable than would be any attempts to make model predictions for the singlet coefficients b_q^0 and c_q^0 .

Second, we cut the loops off at Λ_χ , effectively restricting the virtual Goldstone bosons to have momenta less than the scale of chiral symmetry breaking. An alternative would be to use dimensional regularization and subtract terms proportional to \mathcal{C}_∞ (equivalent to $\overline{\text{MS}}$ renormalization). Since we are interested only in obtaining the scale of the constituent U - and D -quark strangeness current and not in making airtight predictions, either approach would suffice. In order to cut the loops off in a gauge-invariant manner, we employ form factors at the quark-kaon vertices introducing the appropriate seagull graphs as necessary to preserve the WT identities. For simplicity, we use the monopole form of Eq. (43), taking the cutoff parameter $\Lambda \sim \Lambda_\chi$. In effect, we repeat the nonlinear σ -model calculation discussed above for constituent quarks rather than nucleons.⁷

The results of the loop calculation generate effective, constituent quark strangeness current operators

$$\langle Q | \bar{s} \gamma_\mu^s | Q \rangle |_{\text{loop}} \rightarrow \hat{J}_\mu^{\text{strange}} = \hat{\psi} \left[F_{1Q}^{(s)} \gamma_\mu + \frac{iF_{2Q}^{(2)}}{2m_Q} \sigma_{\mu\nu} Q^\nu \right] \hat{\psi}, \quad (47)$$

where Q denotes a constituent quark and $\hat{\psi}$ is a constituent quark field operator. Nucleon matrix elements of $\hat{J}_\mu^{\text{strange}}$ may be computed using quark model wave functions. We choose to employ wave functions in the light-front formalism, since this framework allows one to use the on-shell constituent quark current [the form in Eq. (47)] and allows one to perform boosts along the direction of momentum transfer as needed to properly account for the nucleon’s center-of-mass motion.⁸ Although we are concerned only with the leading, nontrivial Q^2 dependence of the strangeness form factors, it is worth noting that the light-front quark model has successfully reproduced the the nucleon’s EM form factors over a significant range in momentum-transfer [73–75]. We also follow the authors of Ref. [75], who take a tree-level value for the meson-quark coupling $g_A = 1.0$ and an oscillator parameter $\gamma = 1.93 \text{ fm}^{-1}$ and reproduce the nucleon’s isovector axial charge to within 5%. The results are displayed in Table I.

IV. RESULTS AND DISCUSSION

In this section, we give predictions for the nucleon’s strangeness radius and magnetic moment using the three chiral model approaches discussed above. These results are summarized in Table I, where we also include predictions from four previously reported approaches sharing some elements in common with those discussed here. For illustrative purposes, we also display in Fig. 4 the dependence of ρ^s and μ^s on the hadronic form factor cutoff parameter and pseudo-scalar meson mass entering the nonlinear σ -model calculation.

When viewed from the most ‘‘impressionistic’’ perspective, the results in Table I illustrate the wide spread in predictions one encounters among approaches relying on chiral symmetry. Indeed, the strangeness radius and magnetic moment can vary by an order of magnitude and by sign. One ought to conclude that chiral symmetry by itself is not a terribly restrictive input principle when it comes to predicting nucleon strangeness. The reason is essentially that the quantity one wishes to predict is the very quantity one needs in order to make a prediction using CHPT: the SU(3)-singlet vector current. In the absence of experimental information on the latter, the range in one’s predictions can be as wide as the breadth of one’s space of chiral models. From the standpoint of hadron structure theory, this situation is not very satisfying, since one would like to possess a reliable effective-theory framework for interpreting the up-coming measurements of the low-energy properties of the $s\bar{s}$ sea.

Nevertheless, a discussion of the physics input used in each model, along with the attendant model ambiguities, may clarify the elements needed in a more realistic treat-

⁷By choosing the form factor cutoff parameter to be Λ_χ , we introduce no new scale into the problem.

⁸We omit here a discussion of the ambiguities associated with the light-front formalism, such as dynamical effects associated with the transformation from the equal-time framework. These ambiguities are discussed elsewhere in the literature [71,72].

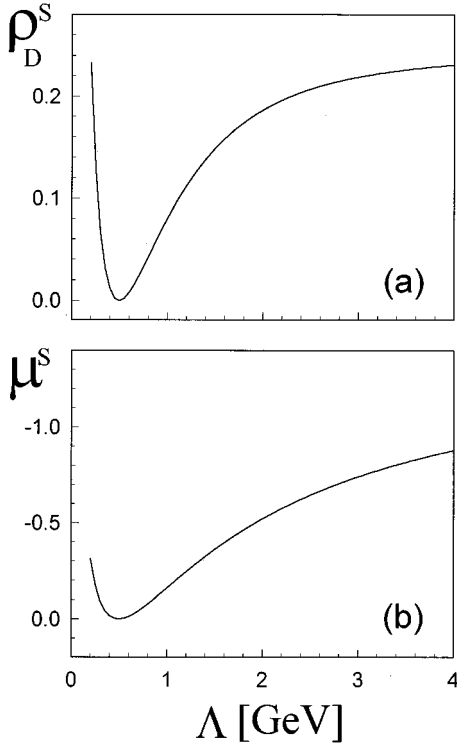


FIG. 4. Nucleon strangeness vector current moments in the nonlinear σ model with hadronic form factors. Dimensionless Dirac strangeness radius (a) and strangeness magnetic moment (b) are shown as functions of the form factor cutoff parameter. To set the scale, note that the nucleon's dimensionless isovector EM Dirac radius is $\rho_D^{T=1} = -4.68$.

ment. To that end, we summarize the logic behind each of these models and point out the primary model uncertainties.

(1) Resonance saturation. Of the models considered here, resonance saturation remains closest in spirit to CHPT while affording, perhaps, the clearest identification of the physics elements included as well as those omitted from the analysis. In the case of the Dirac strangeness radius, these elements may be summarized as follows.

(a) Detailed dispersion theoretic analyses of the isovector charge radius imply that it is dominated by the lowest continuum state (two pions) and the lightest isovector 1^{--} resonance. Formally, the large two-pion continuum contribution results from a left-going branch cut just in the πN scattering amplitude below the two pion threshold [64]. In CHPT, this effect appears in the guise of the leading nonanalytic term ($\ln m_\pi^2/\mu^2$). Contributions from $\pi\pi$ continuum terms analytic in the light quark masses and from the ρ resonance are accounted for by the chiral counterterms, c_\pm , which may be fit to data. In the resonance saturation approach, one retains only the $\ln m_\pi^2/\mu^2$ term from the loop as an indication of the continuum contribution and models the isovector counterterms using the ρ resonance. Although this model overpredicts the isovector charge radius by a factor of 2 [54], the sign and order of magnitude are given correctly. The overprediction appears to result from the omission of nonresonant pion rescattering corrections [56].

(b) One might expect an analogous situation to arise in the isoscalar and strangeness channels, where the lightest con-

tinuum states are the 3π , 5π , 7π , and $2K$ states and the lightest isoscalar 1^{--} vector mesons are the ω and ϕ . Some thought about chiral counting suggests that the multipion contributions ought to be suppressed relative to the $2K$ contribution. To the extent that (i) this suppression holds and that (ii) the total, nonresonant $2K$ contribution to the isoscalar charge radius is no larger than the leading, nonanalytic kaon loop contribution, the isoscalar charge radius would then be dominated by the lightest isoscalar vector mesons, rendering the fit of Ref. [62] quite valid. The results of this fit indicate that the ω and ϕ residues dominate the isoscalar Dirac radius; the contribution from higher mass vector mesons is negligible. Thus, the isoscalar constant $c^{T=0}$ should be given quite reliably by the ω and ϕ contributions.

(c) Knowledge of the ω and ϕ flavor content allows one to translate the ω and ϕ contributions to $c^{T=0}$ into the corresponding contributions to the strangeness constant, c^s . If the nonresonant multipion contributions to the strangeness radius are suppressed with respect to the $2K$ contribution, if the nonanalytic kaon loop contribution [Eq. (29)] accurately reflects the scale of the two-kaon continuum, and if there are no important vector meson effects beyond those of the ω and ϕ , then ρ_D^s ought to be given accurately by resonance saturation model.

One should note that this line of argument avoids the problematic use of assumptions about the strangeness form factors' large Q^2 behavior while incorporating the consistency of the heavy baryon chiral expansion. The logic, nevertheless, may be criticized on several grounds.

First, the resonance saturation model is only partially successful in the case of the nucleon's EM moments, in contrast to the situation with the pion form factor. In the case of the isovector radius noted above, the nonanalytic loop contribution is significantly larger than the experimental value: $\rho_{\text{loop}}^{T=1}/\rho_{\text{expt}}^{T=1} \approx 1.5$ (taking $\mu \approx m_\rho$).⁹ One therefore requires a contribution from $c^{T=1}$ which cancels about 40% of the loop contribution. The ρ meson contribution to $c^{T=1}$, computed using the values of F_V taken from e^+e^- data and G_V determined from fits to NN scattering amplitudes [60] does not give such a cancellation. In fact, a careful analysis of the isovector spectral function for the Dirac form factor, which contains information about both the complete set of $\pi\pi$ continuum and ρ resonance contributions, can be used to extract a value for G_V consistent with the value used in NN scattering studies [63]. Inclusion of the full $\pi\pi$ continuum, and not simply the leading nonanalytic term, appears to be crucial in this case.

Second, a more refined dispersion analysis of the isoscalar spectral functions could reveal important nonresonant multipion and kaon continuum contributions. While the leading, nonanalytic kaon loop contribution to the isoscalar Dirac radius is small (about 15% of the experimental value), one

⁹In the work of Ref. [76], only π loops were considered and the result for $\rho_{\text{loop}}^{T=1}$ is closer to the experimental value. Our result also includes the K -loop contribution. Although the calculation of Ref. [76] was carried out without using the heavy baryon formalism, the result agrees with the chiral log of the heavy baryon calculation. The results for the magnetic moment differ, however.

does not know at present whether this result gives a reasonable estimate for the scale of the full continuum. Indeed, since m_K/Λ_χ is not small, it would not be surprising to find important kaon rescattering corrections which could significantly alter the leading-order nonanalytic result. Should the continuum be significantly larger, the pole analyses of Refs. [61,62,64] would require modification, presumably resulting in significantly different values for the residues. In this case, the ω and ϕ contributions to the strangeness counterterm c^s , obtained via Eq. (42), would be altered. Moreover, the presence of large nonresonant continuum effects in the isoscalar channel would suggest similar effects in the strangeness channel.

Third, higher mass poles could play a more important role in the strangeness form factors than in the isoscalar form factors, as discussed in Refs. [40,41]. Indeed, something beyond the simple ω and ϕ pole approximation would be required to generate a Q^2 dependence for $F_1^{(s)}$ consistent with various scenarios for its asymptotic behavior. At present, one has no knowledge of the couplings G_V , G_T , and F_V associated with higher mass poles, nor does one know their flavor content. Consequently, the associated residues a_V^s , can only be fixed by assuming a particular large- Q^2 behavior for $F_1^{(s)}$.

In general terms, these criticisms apply as well to the model prediction for μ^s . In addition, one must note an inconsistency between the resonance saturation model for b^s and the way in which the constant $b^{T=0}$ has been extracted from the isoscalar data. In the analysis of Refs. [61,62], no continuum contributions were included in the fit to the isoscalar form factors. Such an approximation may be valid in the case of the isoscalar Dirac radius, for which the non-analytic loop contributions represent a reasonably small fraction of the total. The $\mathcal{O}(\sqrt{m_s})$ kaon loop contribution to the isoscalar anomalous magnetic moment, however, is large: $\kappa_{\text{loop}}^{T=0}/\kappa_{\text{expt}}^{T=0} \approx 20$. Chiral perturbation theory therefore requires a large constant $b^{T=0}$ to cancel most of this loop contribution. However, the most reliable information one has on the resonance contributions to the isoscalar magnetic form factor is derived from the fits of Ref. [62], which included no continuum. The residues $b_{\omega,\phi}^{T=0}$ obtained from these fits are small (on the order of $\kappa_{\text{expt}}^{T=0}$) and, therefore, cannot cancel the large kaon loop contribution. In order to remove this inconsistency, one would need a reanalysis of $F_2^{T=0}$ which includes a realistic treatment of the continuum.

While these observations raise questions about the credibility of the resonance saturation model, they also highlight several of the elements needed in a more realistic analysis: (a) better knowledge of the nonresonant continuum contributions to the isoscalar spectral functions, which includes information beyond the leading, nonanalytic terms; (b) a reanalysis of the isoscalar pole contributions in light of (a); (c) a means for including the analytic, nonresonant multipion and kaon continuum contributions to the strangeness form factors; (d) an estimate of the higher-mass (beyond the ω and ϕ) vector meson pole contributions to ρ^s and μ^s ; and (e) a clear understanding of the relationship between the asymptotic behavior of the strangeness form factors and (c) and (d).

(2) Kaon cloud dominance. Kaon cloud dominance mod-

els rely on the ansatz that (i) OZI-allowed processes give the most important contribution to the strangeness form factors; (ii) of the OZI-allowed contributions, the most significant are those involving intermediate states with valence s and \bar{s} quarks; and (iii) the largest effects result from the lightest YK states—especially in the case of ρ^s , which naively reflects the mean square spatial polarization of s and \bar{s} quarks. When implementing this ansatz, kaon cloud dominance models typically (i) rely on chiral symmetry to determine the NYK couplings for pointlike hadrons; (ii) regulate UV divergences in loops by employing form factors at the NYK vertices; and (iii) restrict themselves to one-loop order under the assumption that the one-loop result fairly reflects the scale of full kaon cloud contribution.

While kaon cloud dominance models give a satisfying, albeit simple, intuitive physical picture behind nucleon strangeness, each of the assumptions on which they rely can be challenged.

(a) It is not at all clear that OZI-allowed processes dominate the strangeness form factors. Indeed, the pole analyses discussed above and in Refs. [30,64,40,41], if correct, imply large contributions from the $\phi(1020)$, whose coupling to the nucleon ostensibly involves an OZI-violating mechanism.

(b) It is similarly not clear that only intermediate states containing valence s and \bar{s} quarks give important contributions to the form factors. For example, a 3π intermediate has the correct quantum numbers to contribute to the strangeness vector current matrix element, even though it has no valence s or \bar{s} quarks. Moreover, three pions can resonate to the $\phi(1020)$, which has a 15% branch to a three pion final state (primarily through a $\rho\pi$ channel), and thereby generate a nontrivial contribution. In fact, a simple estimate of the 3π contribution, based on this mechanism, suggests that its contribution need not be smaller than that of YK intermediate states [77].

(c) The recent work of Ref. [39] points out the possibility that higher mass Y^*K^* states may significantly cancel contributions from the lightest YK states (kaon cloud). In that calculation, carried out at one-loop order and using the non-relativistic quark model (NRQM), the authors find that one must include Y^*K^* states at rather high excitation before obtaining a stable result for ρ^s and μ^s . Similarly, calculations carried out using hadronic effective approaches find important contributions from YK^* loops [78]. While one has reason to question the reliability of one-loop results [49], these results nevertheless raise questions about validity of assuming kaon cloud dominance.

(d) The use of chiral symmetry in kaon cloud models is not self-consistent. As noted earlier, these models abandon a well-defined chiral expansion by employing form factors at the hadronic vertices and by retaining both analytic and nonanalytic terms from the one-loop calculation. Terms of the former class are indistinguishable from contributions generated by higher-dimension operators in the chiral Lagrangian. Moreover, higher-order loop graphs may yield analytic terms of the same chiral order as some of the analytic terms retained from the one-loop graphs. A consistent chiral approach would require the inclusion of all analytic contributions of a given order in $1/\Lambda_\chi$. In the absence of such an expansion, one has no principle to justify the omission of rescattering corrections associated with higher-order loops.

In fact, any calculation which retains both analytic and nonanalytic contributions must also include higher-order rescattering effects in order to be consistent with the requirements of unitarity [49].

(e) The choice of hadronic form factor is not unique. In the CBM, for example, the form of the effective $F(k^2)$ is approximately Gaussian rather than monopole as used here. Moreover, the scale of the momentum cutoff is set by the inverse bag radius, which is on the order of a few hundred MeV [32]. The CBM constitutes a chiral model with a different underlying physical picture than the nonlinear σ model, and its parameters can be tuned to produce agreement with at least some of the nucleon's EM form factors. In short, one has no strong phenomenological reason to choose one model—corresponding to one form for $F(k^2)$ —over another; only a model preference.

(f) The prescription for maintaining gauge invariance is also not unique. The one shown above in Eq. (45) is a *minimal* procedure. One may include additional seagull contributions which are purely transverse and, therefore, do not affect the WT identity. The presence of these additional terms may, nevertheless, affect one's results for the form factors.

It is instructive to try and quantify the uncertainty associated with these ambiguities. This effort has been accomplished in Ref. [49], where the numerical impact of rescattering corrections and/or higher-order loops has been estimated using unitarity bounds. In the case of form factor ambiguities [point (e) above], one may attempt to quantify the uncertainty by considering the Λ dependence of the linear and nonlinear σ -model predictions and by comparing these predictions with those of the CBM and CCQM calculations. Turning first to the issue of the cutoff dependence, one may argue about which value of Λ to use. The results quoted in Table I and Ref. [31] for the linear σ model were obtained using the Bonn value, $\Lambda \sim \Lambda_{\text{Bonn}} \sim 1.2$ GeV. According to the fits of Ref. [60], taking $\Lambda \sim \Lambda_{\text{Bonn}}$ optimizes agreement with baryon-baryon scattering data in the one meson exchange approximation. For this choice of Λ , however, the corresponding pion loop contributions to the EM moments are in serious disagreement with the experimental values. In fact, there exists no value of Λ which produces agreement between experiment and the linear σ -model values for the EM moments. The best choice occurs for $\Lambda \approx 5$ GeV. In this case, experiment and the linear σ model agree for $\kappa^{T=1}$ while the prediction for $\rho^{T=1}$ is 60% of the experimental value. Changing Λ from Λ_{Bonn} to $\Lambda \approx 5$ GeV doubles the prediction for μ^s and reduces the prediction for ρ_D^s by 25%.

The choice of Λ in the case of the nonlinear σ model is equally debatable, as a study of the pion-loop contribution to the isovector magnetic moment illustrates.¹⁰ We find no value of the cutoff which reproduces the experimental value. Choosing $\Lambda \sim \Lambda_\chi \sim \Lambda_{\text{Bonn}}$ yields, for example, $\kappa_{\text{loop}}^{T=1}/\kappa_{\text{expt}}^{T=1} \approx 25\%$ (the corresponding ratio for the isovector

Dirac radius is $\rho_{\text{loop}}^{T=1}/\rho_{\text{expt}}^{T=1} \approx 27\%$). Taking the limit $\Lambda \rightarrow \infty$ gives $\kappa_{\text{loop}}^{T=1}/\kappa_{\text{expt}}^{T=1} \approx 54\%$ (the isovector Dirac radius diverges in this limit). One might argue, then, that choosing any value of the cutoff in the range $\Lambda_\chi \leq \Lambda \leq \infty$ would be equally justified—at least for the magnetic moments which are UV finite. As the cutoff is varied over this range, μ^s varies from the value quoted in Table I to $\mu^s = -1.31$. This situation appears to persist in the case of the CBM and CCQM models as well. The authors of Ref. [32] originally found values for the cutoff which optimized agreement with all the nucleon's EM moments. However, a subsequent inclusion of covariantizing seagull graphs changed the magnetic moment predictions by 50% so that an optimum cutoff no longer exists. Consequently, the corresponding predictions for the strangeness moments contains an uncertainty associated with the value of the cutoff.

A comparison between different kaon cloud models reveals a similar degree of ambiguity. We consider first the linear and nonlinear σ models. When one of the baryons is off shell, as is the case in a loop calculation, the structure of the meson-baryon vertices differ in the two models, even though the same monopole form factor was used in both calculations. When one takes $\Lambda \sim \Lambda_\chi \sim \Lambda_{\text{Bonn}}$, the two models give nearly identical predictions for ρ_D^s . One might not be surprised by this result, since in both cases the radius contains a chiral log. At least in the chiral limit, this infrared singularity dominates over contributions analytic in m_K , and it is essentially terms of the latter type which would be responsible for any differences in the two predictions. For $\Lambda \rightarrow \infty$, on the other hand, ρ_D^s diverges in the nonlinear σ model but only doubles in value in the linear σ model. In the case of the strangeness magnetic moments, which contain no infrared or ultraviolet singularities, the model predictions¹¹ differ by a factor of about 1.5 for $\Lambda \sim \Lambda_\chi$ but come into closer agreement for $\Lambda \rightarrow \infty$. Comparing the CBM and σ model ($\Lambda = \Lambda_{\text{Bonn}}$) predictions, one finds CBM gives a 50% larger Dirac radius but a value for μ^s that is a factor of three or four smaller than the linear σ -model prediction.

These comparisons are not definitive. Nevertheless, they suggest a scale for uncertainty in the kaon cloud dominance predictions that amounts to about a factor of 5 or more times the smallest values for $|\rho_D^s|$ and $|\mu^s|$. Moreover, as in the case of the resonance saturation model, a study of the weaknesses of the kaon cloud models highlights important elements which a more realistic calculation should include (i) a method for including higher-order rescattering corrections; (ii) a procedure which avoids the ambiguities associated with hadronic off-shell effects, that is, hadronic form factors and the attendant gauge invariance issues; (iii) an analysis of contributions from as full a set of allowed hadronic intermediate states, including those (such as the 3π state) which contain no valence s or \bar{s} quarks.

(3) Chiral quarks. The insights embodied in the chiral quark model approach are the success of the constituent quark model in describing hadron properties, the picture of a constituent quark as a QCD quark dressed by a cloud of

¹⁰One would not expect the pion loop graphs to produce agreement with the isoscalar moments. As the heavy baryon calculation illustrates, the leading contribution arises from the diagrams where the current is inserted in the meson line. In the case of the pion loops, these diagrams only contribute to the isovector moments.

¹¹The lower value for $|\mu^s|$ in the case of the linear σ model corresponds to $\Lambda = 1.2$ GeV.

$q\bar{q}$ pairs and gluons, and idea that the spontaneous breaking of chiral symmetry in the QCD Lagrangian ought to be reflected by interactions between the Goldstone modes and constituent quarks. In the case of strangeness, the primary assumptions underlying the chiral quark approach are that nucleon's strangeness moments arises from a quark-model average of the constituent quark strangeness radii and magnetic moments and that the latter are generated constituent quark-Goldstone boson interactions. Despite the attractive features of this approach, however, it can be questioned on both conceptual and technical grounds.

From the conceptual standpoint, perhaps the primary difficulty involves an issue of double counting. As noted in Ref. [51], the chiral quark effective theory contains both the pseudoscalar $Q\bar{Q}$ bound states as well as the octet of light pseudoscalar Goldstone bosons. To the extent that the latter are also $Q\bar{Q}$ bound states, the theory contains the same set of states in two different guises. The authors of Ref. [51] argue, based on a simple Goldstone boson- $Q\bar{Q}$ mixing diagram, that the mass of the bound state must be either somewhat greater than Λ_χ , in which case it lies outside the realm of the low-energy effective theory, or infinity, in which case it is unphysical. One would conclude that the Goldstone boson octet is distinct from the lightest $Q\bar{Q}$ states of the theory. A study of meson spectroscopy, however, suggests otherwise. Indeed, the pattern of mass splittings in the BB^* , DD^* , KK^* , and $\pi\rho$ systems is remarkably consistent with the mass splittings in conventional quarkonia between the lightest 3S_1 and 1S_0 $Q\bar{Q}$ states [79]. This pattern strongly suggests that the Goldstone bosons are the lightest $Q\bar{Q}$ bound states of the effective theory [80], in conflict with the conclusions of Ref. [51]. There do exist methods for constructing a chiral quark effective theory which includes mesons as specific degrees of freedom while avoiding the double counting problem (see, e.g., Ref. [81]). However, performing a calculation at this level of sophistication lies beyond the scope of the present study.

A second issue is equally as problematic. As in the case of baryon effective theories, the calculation of the constituent quark strangeness matrix elements employs loops. A consistent chiral expansion requires that one retain from these loops only those terms which cannot be mimicked by tree-level contributions from higher-order terms in the chiral Lagrangian [e.g., Eq. (46)]. Such higher-order Lagrangians come with coefficients which cannot be determined without knowing the strangeness matrix elements themselves. This dilemma is the same one which hampers heavy baryon CHPT as a predictive tool. One is hard pressed to go beyond the leading nonanalytic contributions without invoking additional model assumptions.

As a fall back, one can employ form factors to cut off the loop integrals at a scale Λ_χ as we did in arriving at the numbers in Table I, but price one pays is the presence of all the ambiguities encountered when using hadronic form factors in hadronic loops. Presumably, the spread in predictions for the constituent quark strangeness currents is as broad as are the kaon cloud dominance predictions for the nucleon's strangeness moments. When one considers models other than

the chiral quark model, the situation is even less controlled. For example, the NJL model, which provides an alternative model for the constituent quark strangeness radius, gives a value for ρ_S^s that has the opposite sign from the chiral quark prediction and about 40% of the magnitude [33].

Finally, when one compares the predictions for chiral quark model and nonlinear σ -model predictions for ρ_D^s , one finds that the former is a factor of five larger than the latter. In both cases, the form for the meson-fermion vertex is the same, including the approximate value of the form factor cutoff. One faces the question as to whether these two calculations give independent contributions which should be added, or whether there is some overlap between the two. One might argue in favor of the second possibility by noting that at the quark level, a loop involving a kaon and strange baryon intermediate state contains diagrams in which a constituent quark fluctuates into a freely propagating S quark and kaon (i.e., the chiral quark model contribution) plus others in which the S -quark interacts with the other intermediate-state constituent quarks. More generally, a simple dimensional arguments suggest that the mean lifetime of a virtual $s\bar{s}$ pair is not so short compared with typical hadronic lifetimes that one may neglect collective (i.e., hadronic) effects involving the nucleon's strange sea. It would appear that a simple quark model average of the U - and D -quark strangeness moments omits such hadronic processes.

(4) Other model approaches. For completeness, we comment briefly on the other model approaches listed in Table I. Pure vector meson dominance models, such as the three pole model of Ref. [30], omit all nonresonant Goldstone boson continuum contributions. This practice is not justified by any deep theoretical arguments, but rather by one's experience in the isoscalar channel where an acceptable χ^2 is obtained with a three-pole only fit. The one-loop heavy baryon calculation implies, however, that the continuum contributions need not be negligible in the strangeness sector. Moreover, the prediction of Ref. [30] relies on questionable assumptions about the asymptotic behavior of the form factors. The hybrid model of Refs. [33,34] attempts to model both resonant and nonresonant kaon cloud contributions in a self-consistent manner while avoiding the problematic assumptions regarding asymptopia. In treating the two-kaon continuum, however, the hybrid model still invokes hadronic meson-baryon form factors to cutoff the loop integrals for momenta above Λ_χ . Moreover, other potentially important multimeson continuum contributions are not taken into account. Consequently, the hybrid model suffers from the same ambiguities discussed in relation to the other kaon cloud dominance models.

Experimental Implications. In light of the variety of physical processes which may contribute to the strangeness form factors, as well as the ambiguities and oversimplifications which each model entails, is there any insight which a study of chiral models might yield when compared with future experimental results? At the most general level, measurements of μ^s and ρ^s will determine the chiral counterterms, b_s and c_s . Insofar as the nonanalytic loop contributions and counterterms reflect the presence of "long-distance" and "short-distance" physics (as is the standard lore in CHPT), such a determination would indicate the rela-

tive importance of these two types of physics in shaping the low-energy structure of the $s\bar{s}$ sea.

It would be desirable, however, to make more specific statements about the hadronic mechanisms contributing to the strangeness matrix elements. In this respect, our analysis of the chiral model shortcomings may shed some light. To that end, some observations about the magnitudes and signs of their predictions is in order. In the case of μ^s , all of the models, except for the resonance saturation model, give $\mu^s \sim -\mu^{T=0}$. The large positive value for μ^s in the resonance saturation model results from a large loop contribution—enhanced by a factor of $\pi(m_K/\Lambda_\chi)$ —and the questionable absence of correspondingly large vector meson terms. As for the strangeness radius, all of the calculations containing kaon loops (except resonance saturation) give the same sign for ρ^s and magnitudes which vary by a factor of 5. The sign corresponds to the naïve expectation derived from the kaon cloud picture in which the kaon, containing the \bar{s} quark, lives farther, on average, from the nucleon’s center of mass than does the Λ , where the s quark resides. The pole and resonance saturation models, however, give strangeness radii having much larger magnitudes and the opposite sign. The latter results follow from the fits of Refs. [61,62] which yield a large ϕNN coupling. Note that in the case of the resonance saturation model, the large ϕ -pole contribution to ρ_D^s is cancelled to some extent by the continuum term (loops), whereas in the pure pole model, the ϕ contribution is cancelled to an even greater degree by the questionable V' residue. An experimental result consistent with resonance saturation value ρ_D^s would suggest that resonant t -channel kaon and multipion rescattering (poles) is the most important physics behind the strangeness radius. A significantly smaller result, or one having the opposite sign, would imply the presence of large continuum contributions going beyond one-loop order and/or important higher-mass resonance terms.

How might the various parity-violating electron scattering experiments do in terms of sorting out among these scenarios? The SAMPLE experiment at MIT-Bates [2,3] and “ G^0 ” experiment planned for TJNAF [4] anticipate a determination of μ^s with an error bar of ± 0.2 . At this level of precision, these experiments could confirm the presence of a large strangeness magnetic moment (on the order of the resonance saturation prediction) or rule out the remaining predictions. It would be difficult for the SAMPLE and G^0 measurements to confirm any of these remaining predictions without significantly better precision. As far as the strangeness radius is concerned, one anticipates a determination of ρ_S^s with an error of $\approx \pm 1.0$ from the Hall A and C experiments at TJNAF [4,6]. These experiments could see a strangeness radius at the level of the pole and resonance saturation predictions and, at best could rule out (but not confirm) the remaining entries in Table I. It appears that a “second generation” of parity-violation experiments, designed to reduce the error in the strangeness moments, would be useful in pointing to the mechanisms responsible for their magnitudes as signs.

Parenthetically, we note that forward angle parity-violating electron scattering experiments with a proton target [4,6,7] are sensitive to the linear combination $\rho_S^s + \mu^p \mu^s$ where $\mu^p \approx 2.79$ is the proton’s magnetic moment [1,10]. It

has been suggested that a determination of this linear combination is useful as a “first pass” probe of the nucleon’s strangeness vector current. Naïvely, a one might conclude that a small result for this quantity would indicate small magnitudes for $G_E^{(s)}$ and $G_M^{(s)}$. In the case of the resonance saturation model, for example, prediction for $\rho_S^s + \mu^p \mu^s$ is an order of magnitude smaller than the predicted values of either ρ_S^s or μ^s alone, owing to a cancellation between the two terms. Similarly serious cancellations occur in the case of several of the other model predictions. One ought to be cautious, therefore, about drawing strong conclusions from a forward angle measurement alone. A pair of forward and backward angle measurements, allowing for separate determinations of μ^s and ρ^s , would be more relevant to the comparison of model predictions.

V. SUMMARY

In this study, we sought to delineate the extent to which chiral symmetry can be used to arrive at credible predictions for the nucleon’s strangeness vector current form factors. Since CHPT has proven quite useful in other contexts, it is timely to analyze its usefulness in the case of nucleon strangeness. Moreover, since the role of the $s\bar{s}$ sea in the nucleon’s low-energy properties is of considerable interest to the hadron structure community, and since significant experimental effort is being devoted to measuring the nucleon’s strange quark form factors, one would like to possess an effective theory framework in which to understand the strong interaction dynamics behind the numbers to be extracted. Ideally, CHPT would have provided such a framework. We hope to have convinced the reader that nucleon strangeness [or, equivalently, the SU(3)-singlet channel] presents barriers to the applicability of chiral symmetry not present in other cases where symmetry has proven more useful. To reiterate: the reason for this difficulty is that the quantity one wishes to predict—the strangeness [or SU(3)-singlet] vector current matrix element—is the same quantity one needs to know in order to make a prediction.

Consequently, we turned our attention to chiral models. We explored three such model approaches as a representative sampling: a resonance saturation model for the unknown low-energy constants arising in CHPT; kaon cloud dominance models; and models in which chiral symmetry is used to obtain the strangeness currents of constituent U and D quarks. These different approaches yield a wide range of predictions for the nucleon’s strangeness radius and magnetic moment. This situation is not surprising, since none of the approaches relies solely on the underlying symmetries of low-energy QCD, but invokes, in addition, various model assumptions. We have argued that the set of physical processes which may influence the strangeness form factors is too broad to be encompassed by any one of these models. As a result, models which emphasize different subsets of these processes can lead to rather different predictions. A more realistic and comprehensive analysis should incorporate the complete range of physically significant effects, including the full set of mesonic continuum contributions and not sim-

ply the lowest-lying YK states, rescattering corrections to the leading nonanalytic terms, resonances, both OZI-violating as well as OZI-allowed processes, the requirements of perturbative QCD regarding the large Q^2 behavior, and so on. In addition, such an analysis should avoid some of the uncontrolled approximations and ambiguities which plague chiral models, such as a truncation at the lowest loop order, introduction of hadronic form factors, double counting of quark and hadronic degrees of freedom, etc. In this regard, the use of dispersion relations appears to be a promising approach [49]. Such an analysis, carried out in tandem with precise measurements of $G_E^{(s)}$ and $G_M^{(s)}$, could elucidate the low-energy structure of the $s\bar{s}$ sea.

ACKNOWLEDGMENTS

We wish to thank J. L. Goity, R. L. Jaffe, X. Ji, D. Leinweber, U. Meissner, and N. Isgur for useful discussions and T. Schaefer for raising the question about the resonance saturation model for the chiral counterterms. We also thank M. Frank and H.-W. Hammer for their critical reading of the manuscript. This work was supported in part by funds provided by the U.S. Department of Energy (DOE) under Contract Nos. DE-AC05-84ER40150, DE-FG06-90ER40561, and DE-FG02-95-ER40907. M.R.-M. was also supported by the National Science Foundation National Young Investigator Program.

-
- [1] M. J. Musolf *et al.*, Phys. Rep. **239**, 1 (1994).
 [2] MIT-Bates Report No. 89-06, 1989.
 [3] MIT-Bates Report No. 94-11, 1994.
 [4] TJNAF Report No. PR-91-017, 1991.
 [5] TJNAF Report No. PR-91-004, 1991.
 [6] TJNAF Report No. PR-91-010, 1991.
 [7] Mainz Report No. A4/1-93, 1993.
 [8] See, e.g., R. McKeown and M. J. Musolf, in *Symmetries and Fundamental Interactions in Nuclei*, edited by W. C. Haxton and E. M. Henley (World Scientific, Singapore, 1995), and references therein.
 [9] Los Alamos Report No. 1173.
 [10] M. J. Musolf and T. W. Donnelly, Nucl. Phys. **A546**, 509 (1992); **550**, 564(E) (1992).
 [11] G. T. Garvey *et al.*, Phys. Lett. B **289**, 249 (1992); Phys. Rev. C **48**, 1919 (1993).
 [12] C. J. Horowitz *et al.*, Phys. Rev. C **48**, 3078 (1993).
 [13] M. B. Barbaro *et al.*, INT Report No. INT/DOE/ER/40561-243-INT96-00-112, 1996.
 [14] K.-F. Liu, University of Kentucky Report No. UK/95-11, 1995, and references therein.
 [15] D. B. Leinweber, Phys. Rev. D **53**, 5115 (1996).
 [16] T. P. Cheng, Phys. Rev. D **13**, 2161 (1976); J. Gasser, H. Leutwyler, and M. E. Sainio, Phys. Lett. **168B**, 105 (1986).
 [17] EMC Collaboration, J. Ashman *et al.*, Nucl. Phys. **B328**, 1 (1989).
 [18] E142 Collaboration, P. L. Anthony *et al.*, Phys. Rev. Lett. **71**, 959 (1993).
 [19] SMC Collaboration, B. Adeva *et al.*, Phys. Lett. B **302**, 533 (1993).
 [20] SMC Collaboration, D. Adams *et al.*, Phys. Lett. B **329**, 399 (1994).
 [21] E143 Collaboration, K. Abe *et al.* Phys. Rev. Lett. **74**, 346 (1995).
 [22] J. Gasser, H. Leutwyler, and M. E. Sainio, Phys. Lett. B **253**, 252 (1991).
 [23] E. Jenkins and A. Manohar, Phys. Lett. B **255**, 558 (1991); **259**, 353 (1991).
 [24] J. Dai, R. Dashen, E. Jenkins, and A. Manohar, UCSD Report No. PTH 94-19, 1995.
 [25] B. Ehrnsperger and A. Schafer, UFTP Report No. 377-1994, 1994.
 [26] J. Lichtenstadt and H. Lipkin, Tel Aviv Report No. TAUP-2244-95, 1995.
 [27] See, e.g., S. Capstick, *Constituent Quark Models of Baryon Structure and Strong Decays and A Comparison with Experimental Results, and Outstanding Issues in Baryon Physics*, in Proceedings of the NATO Advanced Study Institute on Hadron Spectroscopy and the Confinement Problem, edited by D. V. Bugg, 1995 (University of London, London, 1995).
 [28] CCFR Collaboration, A. O. Bazarko *et al.*, Z. Phys. C **65**, 189 (1995); CCFR Collaboration, S. A. Rabinowitz *et al.*, Phys. Rev. Lett. **70**, 134 (1993).
 [29] We are grateful to J.W. Negele for clarifying this issue for us.
 [30] R. L. Jaffe, Phys. Lett. B **229**, 275 (1989).
 [31] M. J. Musolf and M. Burkardt, Z. Phys. C **61**, 433 (1994).
 [32] W. Koepf, S. J. Pollock, and E. M. Henley, Phys. Lett. B **288**, 11 (1992); W. Koepf and E. M. Henley, Phys. Rev. C **49**, 2219 (1994).
 [33] H. Forkel *et al.*, Phys. Rev. C **50**, 3108 (1994).
 [34] T. Cohen, H. Forkel, and M. Nielsen, Phys. Lett. B **316**, 1 (1993).
 [35] N. W. Park, J. Schechter, and H. Wiegel, Phys. Rev. D **43**, 869 (1991).
 [36] S.-T. Hong and B.-Y. Park, Nucl. Phys. **A561**, 525 (1993).
 [37] S. C. Phatak and S. Sahu, Phys. Lett. B **321**, 11 (1994).
 [38] H. Ito, Phys. Rev. C **52**, R1750 (1995).
 [39] P. Geiger and N. Isgur, Phys. Rev. D **55**, 299 (1997).
 [40] M. J. Musolf, Proceedings of the Eleventh Student Workshop on Electromagnetic Interactions, Bosen, Germany 1994.
 [41] H. Forkel, Prog. Part. Nucl. Phys. **36**, 229 (1996); H. Forkel, Report No. hep-ph/9607452, 1996.
 [42] H.-W. Hammer, Ulf-G. Meissner, and D. Drechsel, Phys. Lett. B **367**, 323 (1996).
 [43] J. Donoghue, E. Golowich, and B. Holstein, *Dynamics of the Standard Model* (Cambridge University Press, Cambridge, 1992).
 [44] *Proceedings of the Workshop on Effective Theories of the Standard Model*, edited by U.-G. Meissner (World Scientific, Singapore, 1992).
 [45] E. Jenkins *et al.*, Phys. Lett. B **302**, 482 (1993).
 [46] M. N. Butler, M. J. Savage, and R. P. Springer, Phys. Rev. D **49**, 3459 (1994).
 [47] M. K. Banerjee and J. Milana, University of Maryland Report No. UMPP 96-19, hep-ph/9508340, 1995.

- [48] T. D. Cohen, Phys. Lett. B **359**, 23 (1995).
- [49] M. J. Musolf, H.-W. Hammer, and D. Drechsel, Phys. Rev. D **55**, 2741 (1997).
- [50] H. Georgi, *Weak Interactions and Modern Particle Theory* (Benjamin-Cummings, Menlo Park, 1984), Chaps. 5 and 6.
- [51] A. Manohar and H. Georgi, Nucl. Phys. **B234**, 189 (1984).
- [52] R. G. Sachs, Phys. Rev. **126**, 2256 (1962).
- [53] In Ref. [45], a normalization to m_N rather than Λ_χ was employed for the EM anomalous magnetic moment Lagrangian and the notation μ_D and μ_F , rather than b_+ and b_- , was used for the coefficients of the commutator and anticommutator terms, respectively.
- [54] M. J. Ramsey-Musolf, unpublished.
- [55] In the analysis of Ref. [45], a fit to the entire baryon octet was performed. For illustrative purposes, however, we need consider only the nucleons. In the case of the charge radii, there exist no measurements for the strangeness $\neq 0$ octet baryons.
- [56] P. Federbush, M. L. Goldberger, and S. B. Treiman, Phys. Rev. **112**, 642 (1958).
- [57] G. Ecker *et al.*, Phys. Lett. B **223**, 425 (1989).
- [58] G. Ecker *et al.*, Nucl. Phys. **B321**, 311 (1989).
- [59] J. J. Sakurai, *Currents and Mesons* (University of Chicago Press, Chicago, 1969).
- [60] B. Holzenkamp, K. Holinde, and J. Speth, Nucl. Phys. **A500**, 485 (1989).
- [61] H. Genz and G. Höhler, Phys. Lett. **61B**, 389 (1976).
- [62] G. Höhler *et al.*, Nucl. Phys. **B114**, 505 (1976).
- [63] G. Höhler and E. Pietarinen, Nucl. Phys. **B95**, 210 (1975), and references therein.
- [64] P. Mergell, U.-G. Meissner, and D. Drechsel, Nucl. Phys. **A596**, 367 (1996).
- [65] H. A. Bethe and F. deHoffman, *Mesons and Fields* (Row and Peterson, Evanston, 1955), Vol. II.
- [66] T. Hatsuda, Phys. Rev. Lett. **65**, 543 (1990).
- [67] T. Meissner, Phys. Lett. B **340**, 226 (1994).
- [68] D. B. Kaplan and A. Manohar, Nucl. Phys. **B310**, 527 (1988).
- [69] Y. Nambu and G. Jona-Lasinio, Phys. Rev. **124**, 246 (1961); **124**, 255 (1961).
- [70] One may wish to compare the expression in Eq. (46) with the magnetic moment term in the chiral quark Lagrangian of Ref. [51]. The latter contains an additional factor of m/Λ_χ in order to make explicit the chirality-violating character of the magnetic moment interaction. We choose instead a normalization which goes over to the form of Eq. (11) in the heavy quark limit. For simplicity, we have also ignored isospin-violating corrections which break the constituent quark EM magnetic moment relation $\mu_U = -2\mu_D$.
- [71] V. A. Karmanov and A. V. Smirnov, Nucl. Phys. **A575**, 520 (1994).
- [72] P. L. Chung, F. Coester, and W. N. Polyzou, Phys. Rev. C **37**, 2000 (1988).
- [73] P. L. Chung and F. Coester, Phys. Rev. D **44**, 229 (1991).
- [74] S. J. Brodsky and F. Schlumpf, Phys. Lett. B **329**, 111 (1994).
- [75] I. G. Aznauryan, A. S. Bagdasaryan, and N. L. Ter-Isaakyan, Yad. Fiz. **36**, 1278 (1982) [Phys. At. Nucl. **36**, 743 (1982)].
- [76] J. Gasser, M. E. Sainio, and A. Svarc, Nucl. Phys. **B307**, 779 (1988).
- [77] H.-W. Hammer and M. J. Ramsey-Musolf, INT Report No. DOE/ER/40561-317-INT97-00-169, hep-ph/9703406.
- [78] L. L. Barz, H. Forkel, H.-W. Hammer, F. S. Navarra, M. Nielsen, and M. J. Ramsey-Musolf, unpublished.
- [79] N. Isgur, TJNAF Report No. TH-92-31, 1992.
- [80] N. Isgur, private communication.
- [81] M. R. Frank, P. C. Tandy, and G. Fai, Phys. Rev. C **43**, 2808 (1991).